ON THE WAVE MODE OF SUBSECOND PULSES IN THE cm-RANGE

N. S. MESHALKINA[1], A. T. ALTYNTSEV[1], R. A. SYCH[1], G.P. CHERNOV[2] and YAN YIHUA[3]

[1]*Institute of Terrestrial Magnetism, Ionosphere and Radio Wave Propagation, Troitsk, Russia (e-mails: nata@iszf.irk.ru; altyntsev@iszf.irk.ru; sych@iszf.irk.ru)*

[2]*Institute of Terrestrial Magnetism, Ionosphere and Radio Wave Propagation, Troitsk, Russia (e-mail: gchernov@izmiran.troitsk.ru)*

[2]*National Astronomical Observatories, Chinese Academy of Sciences, Datun Road A20, Chaoyang District, Beijing 100012, China (e-mail: yyh@bao.ac.cn)*

(Received 15 December 2003; accepted 2 February 2004)

Abstract. In this paper we determined the wave mode of subsecond pulses (SSP). We used the data on pulses with the degree of polarization over 30%, with the sources located at −60 to +60 deg from the central meridian, for the period 2000–2002. The superposition of SSRT radio maps and MDI magnetograms has shown that radio SSP sources are typically located near the polarity inversion line of the active region magnetic field. Such an arrangement indicates that SSP sources are located at the tops of magnetic loops. The ordinary mode of electromagnetic radiation is recorded in SSP sources located from the inversion line by no less than about 10 arcsec.

1. Introduction

The development of mechanisms to explain solar millisecond radio bursts has been an area of intense research activity for more than two decades. SSP bursts have been known as intense pulses of duration less than one second that are superposed on broadband continuum emission of much longer duration. It is generally agreed that the study of SSP will give insight into the elementary processes taking place in the flaring region, providing a effective tool for diagnostic on particle acceleration, propagation and trapping (e.g., Benz, 1986; Aschwanden, 2002).

The fine temporal structures appear in many different spectral forms varying vastly in bandwidth, polarization and frequency drift, and a number of emission mechanisms was developed for different plasma parameters in the SSP source. But until now it is not clear which emission mechanism corresponds to the observed fine structure. The most interesting kinds of SSP events are pulses with a very high degree of circular polarization (up to 100%), which emission can generally be coherent and excited by non-thermal electrons. Coherent means here that the radiation is not emitted by individual particles, but some electron population formed in a plasma wave. Very polarized emission can be generated at frequencies close to oscillations in plasma eigenmodes which include oscillations at plasma frequency and electron plasma cyclotron frequencies (e.g., Zhelezniakov, 1969).

Solar Physics **0:** 1–15, 2003.

An essential element in obtaining a physical understanding and identifying the generation mechanism of these events is to establish whether we are dealing with ordinary (O-) or extra-ordinary (E-) wave mode. To do this we need information on the magnetic structure of the flaring region, and the position of the source of the emission within that structure. The radio sources with magnetic field of negative polarity (S) and emitting the extraordinary mode are left circularly polarized, and *vice versa*. The lack of data in this area is the main cause of the current uncertainty in identification of the wave modes.

In the absence of direct positional measurements of the accuracy required to locate the source within the flaring region, two empirical rules have been used: the 'Leading Spot Rule', and the 'Nearest Spot Rule'. The first suggests that the vertical component of the radio source is the same direction as in the leading spot of the region; whereas the second makes the same assumption for the spot nearest the flare, associated with SSP event. The most efforts were made to determine of the wave mode (X- or O-mode) for spikes and drift bursts. First events are narrow band pulses of short duration, second ones are the type III-like events with the narrow instant band and pronounced frequency drift. The results reported to date are inconclusive.

Dulk (1985) carried out an analysis of type III bursts. Emission can sometimes be observed at both the fundamental and second harmonic of the plasma frequency, although at the higher frequencies (≥ 100 MHz) it seems that only harmonic radiation is usually present. The fundamental components were moderately polarized ($\approx 30\%$), while the harmonic components were only slightly polarized ($\approx 12\%$), both in the O-mode sense.

Benz and Güdel (1987) examined events (200–1100 MHz) accompanied by the fine structures in the low-frequency part of the spectrum. The Leading Spot Rule was used to determine the dominant mode: in 10 events of 13, it was the O-mode. Usually, the polarization direction in the spikes and accompanying type III bursts was the same.

However, the analysis made by Güdel and Zlobec (**?**) using an extensive sample of Zurich data in the range 100–3000 MHz gave an opposite result: in 98% of the events, the rotation direction of the polarization vector in the spikes and corresponding type III bursts was opposite in sign; the degree of polarization of the spikes is higher than that in type III bursts. According to the Leading Spot Rule, 68% of the spikes turn out to be X-polarized (71% of type III bursts, O-polarized), whereas in the case of using the Nearest Spot Rule, a statistical sample showed that 79% of spikes are X-polarized (79% for type III bursts).

Measurements of spatial characteristics of drifting burst sources are made available, for the first time, through a combined analysis of the data from the Siberian Solar Radio Telescope (Smolkov *et al.*, 1986; Altyntsev *et al.*, 2003a; Grechnev *et al.*, 2003) operating at the frequency of about 5.7 GHz, and from the National astronomical observatory of China (NAOC) spectropolarimeter (Fu *et al.*, 1995; Ji *et al.*, 2003) for the frequency range 5.2–7.6 GHz. The reception band of an

individual frequency channel of the NAOC spectropolarimeter is 20 MHz, and the temporal resolution is 5.9 ms.

Our analysis has shown that all events with fine temporal structure can be separated into different types, having a different origin: narrow-band driftless bursts referred to as spike-like bursts, bursts with a drift, and broad band bursts encompassing a broad frequency band.

The SSRT (operating at 5.7 GHz) recorded about 100 bursts with a subsecond duration (SSP) for the period 2000–2003.

A statistical processing of these bursts recorded before 2003 was carried out by Lesovoi and Kardapolova (2003). They showed that the circular polarization of the SSP is usually opposite in sign to the associated microwave bursts. So, they determine the SSP emission in the ordinary sense, because the background burst appeared mostly due to gyrosinchrotron emission of nonthermal electrons, and it is polarized at the SSRT operating frequency in the extraordinary mode.

The objective of our paper is to determine the emission mode using the simultaneous data with the spatial and spectral resolution, and magnetograms (MDI/SOHO).

The paper is organized as follows. Section 2 outlines the instrumention, Section 3 considers methods of observation and data recording, and instrumentation data processing, Section 4 deals with results of observation and the subsequent analysis. The statistical results of the study and the discussion are presented in Section 5. Section 6 contains general conclusions.

2. Instrumentation

The Siberian Solar Radio Telescope (SSRT) is a crossed radio interferometer, consisting of two lines of antennas: east-west (EW), and north-south (NS), operating in the frequency range 5.67–5.79 GHz (Smolkov *et al.*, 1986; Grechnev *et al.*, 2003).

In this study we used continuous series of solar images obtained in both the additive and correlative operating modes of the instrument. The time interval between separate images of the solar disk varied in the range 2–3 min and depended on the hour angle of the observing time and on solar declination.

The time taken to record the information for a full two-dimensional image is too large (every 2–3 min) to be feasible for observing sub-second events, whereas one-dimensional scans can be made in a much shorter time (every 14 ms). Therefore, in this experiment, the EW and NS arrays were used separately to produce simultaneous, orthogonal one-dimensional scans.

Time profiles of radio flux variation in the intensity ($I = R + L$) and circular polarization ($V = R - L$) channels is posted on a regular basis, on the site of the ISTP Radio astronomical observatory:

http://SSRT.izsf.irk.ru/SSRT/ftevents.html in the SSRT database.

Two-dimensional images were used to align the SSRT images and maps in other emissions. The fine temporal structure of flare bursts was recorded by the EW and NS arrays separately to provide one-dimensional images (scans) of the solar disk.

The methods for analyzing one-dimensional solar images were described by Altyntsev *et al.* (2003a). The SSRT receiving system is represented by the acousto-optic receiver in the 120 MHz frequency band featuring 250 frequency channels which correspond to the fans of knife-edge beams for the NS and EW arrays, respectively. The signal at each frequency corresponds to the emission from a narrow strip on the solar disk whose position and width depend on the frequency. This dependence is determined by the time of observation, and the type of array. The beam widths were down to 15 arc sec for one-dimensional scans, and depend on the array and local time of observation. With the small size of microwave burst sources, they are recorded by the SSRT in a narrow band not exceeding 5 MHz.

Signals from all channels are recorded simultaneously and generate a one-dimensional distribution (scan) of solar radio brightness every 14 ms. The components of the circular polarization (R and L) are recorded successively within the interval of 7 ms duration each. To obtain images in the intensity ($I = R + L$) or circular polarization (V=R-L) channels, the polarization components (R-right-handed, and L-left-handed) were summed together or subtracted respectively.

Our analysis used: time profiles in intensity and polarization (SSRT, 5.7 GHz, 14 ms resolution), 2D maps from the SSRT (every 2–3 min with a resolution of up to 21 arc sec), scans with a resolution of up to 15 arcsec; spectra in the range 5.2–7.5 GHz (data from the NAOC radio polarimeters, 5.9 ms resolution), and magnetograms (MDI/SOHO).

3. Observations and Data Reduction

To determine the emission mode we must determine the direction of magnetic field vector and polarization in the SSP source. The procedure of processing observational data from the SSRT can be divided into several stages.

At the first stage time profiles of the burst flux are calculated from recorded data in the additive operating mode of the SSRT by integrating over the one-dimensional response of the burst region. Then we found the time of SSP maximum.

The second stage includes constructing two-dimensional images of the full solar disk during the burst. The radio map closest in time to the SSP occurrence was selected.

Also, taking into account the mean time of obtaining a single image of about 3 min, the accuracy of time referencing to the event was less than 1.5 min. Taking into account the low level of the SSRT beam sidelobes, radio maps of burst sources were applied without the cleaning procedure.

Figure 1 shows the solar images obtained in different operating modes of the SSRT. The upper panels show 2D SSRT images in the additive and correlation

mode. The circle represents the active region where the SSP occurred. Top left – simultaneous projections of the EW and NS scans are shown at the time of the 2D radio image -û top right. The visible sources 1, 2, and 3 are marked, respectively, in the three figures. The bottom panels show the temporal development of the 1D scans, obtained with the linear EW (bottom left) and NS interferometers (bottom right) with the time shift removed. The black box indicates the time and 1D position of the SSP. The ordinate shows the time (duration of the segment of 52 s shown in the figure), and the abscissa indicates the frequency acousto-optical receiver – 1D position.

As pointed out above, the signal is recorded concurrently from two projections with the EW and NS lines thus making it possible to superimpose on the two-dimensional image one-dimensional responses of the SSP source at different scan angles.

Working with a large dataset of homogeneous observational material, represented as the sum of signals (additive mode) or their multiplication (correlation mode), we are able to confront them unambiguously. This provides a one-dimensional distribution which can be used to deduce spatial changes occurring in the source, at 14 ms intervals. On the other hand, with the closest (in time) two-dimensional map of the burst source, by superimposing the recordings in two projections, we obtain the spatial referencing of the SSP emission maximum. Such a capability of the SSRT operation provided an exact identification of SSP sources and made it possible to trace their moving in space.

We consider the localization technique for sources of subsecond pulses relative to the magnetic field structure in the flaring region of the 21 August 2002 event, for example. There was a flare of class C 5.0 in NOAA 0069, position S11 W45 (Figure 3). The scan angle, measured from the Sun's polar axis, was 90.42° for NS, 14.08° for EW. The intersection point of 1D scan projections passing through the source emission maximum gives us its location on the two-dimensional map. This is shown in Figure 2 (top): the correlation map of the burst source with two scans made at different instants of time: prior to (background burst) and during the SSP, and for different projections.

The intersections of the lines, shown by crosses, indicate the location of the SSP source and of the background burst.

We used MDI magnetograms (soi.stanford.edu/magnetic/index5.html). To determine the magnetic field configuration in the active region where the SSP occurred, we used the superposition of two-dimensional maps from the SSRT (pixel size – 2.4555 arc sec pix^{-1}) on the magnetic field map (pixel size – 1.78 arc sec pix^{-1}) (Figure 2). We selected the magnetograms that were the closest to the occurrence time of the SSP. The superposition was made by taking into account the different scales of the maps, their centering, and for solar differential rotation for the difference time. The accuracy of aligning was as high as 10 arc sec (Figure 2).

Data on the AR's magnetic class were presented in daily reports on solar activity available from: www.sec.noaa.gov/Data/solar.html. Our analysis shows that the

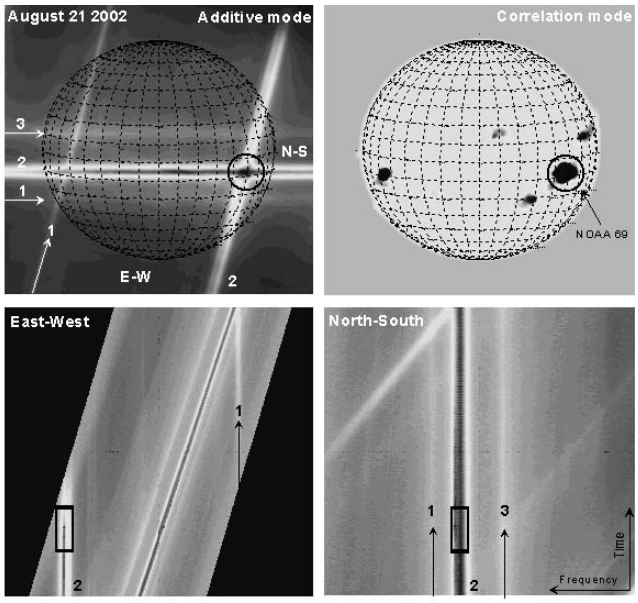

Figure 1. Top: two-dimensional SSRT maps in the additive (*left*) and correlation modes (*right*). *Bottom:* sequence of the one-dimenshional records for NS and EW, respectively.

events have a magnetic configuration of different types. The largest number (8 out of 18) of the selected events has a $\beta\gamma$-configuration, the bipolar complex poles of the active region are insufficiently well separated or the poles include small opposite-polarity sunspots; 5 out of 18 have a $\beta\gamma\delta$-configuration – the opposite-polarity sunspots (umbrae) lie inside a common penumbra.

Our analysis shows that the background sources are characterized by a bipolar configuration in polarized emission. The intensity maximum source positions of background bursts and SSP do not coincide. In some cases the difference is 1 arcmin.

4. Results of Observations

Results of data analysis for 18 events are presented in Table 1, Figure 5, and Figure 6.

To identify the model for the mechanisms of SSP generation, it is important to have data on dynamic spectra. Our analysis used dynamic spectra from the radio polarimeters of the National Astronomical Observatory of China.

We observed fine temporal structure represented by subsecond bursts of three types: narrow-band driftless bursts referred to as spike-like bursts (7 out of 18)(band width 0.15–0.7 GHz); with a drift on the order of -12.8 GHz s^{-1} to 20 GHz s^{-1} classed as type III-like (3 out of 18) (total bandwidth 0.4–1.2 GHz), and broad

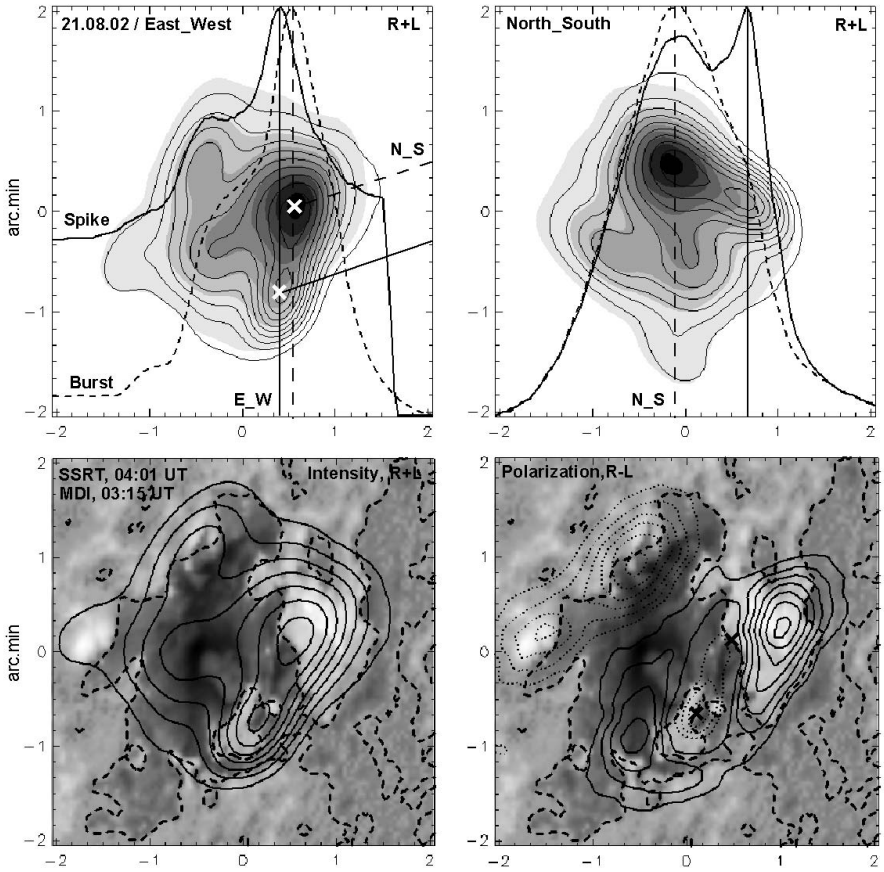

Figure 2. Top: the SSP source position relative to the background burst from 1D scans for NS and EW, respectively (*solid line* – 1D scan of SSP source (time 04:02:32), *dashed line* – 1D scan of background burst (time 04:02:51) (these scans were normalized), contour – 2D intensity (the nearest to SSP, time 04:03:25), shading – intensity (2D map of background burst – time 04:01:09). *Bottom:* superposition of 2D SSRT maps (contour left - Intensity of the nearest 2D map to the SSP – time 04:03:25), contour right – polarization) on the MDI magnetograms (*white color* – N, black – S, *dashed line – neutral line*).

band bursts encompassing the entire frequency band (2 out of 18). Examples of spike and broand band burst are in Figure 4. The verification for broad band burst using the data from the Nobeyama Polarimeters (1.0−35.0 GHz) showed that there was response on 1.0; 2.0; 3.75 GHz, i.e., SSP's are broad band ones. SSPs have a different spectral features and, hence, a different origin.

For one-third of the events it was not possible to analyze dynamic spectra (the response was too weak for the NAOC radio polarimeters, or no observations were made at that time). A verification for these events using the data from the

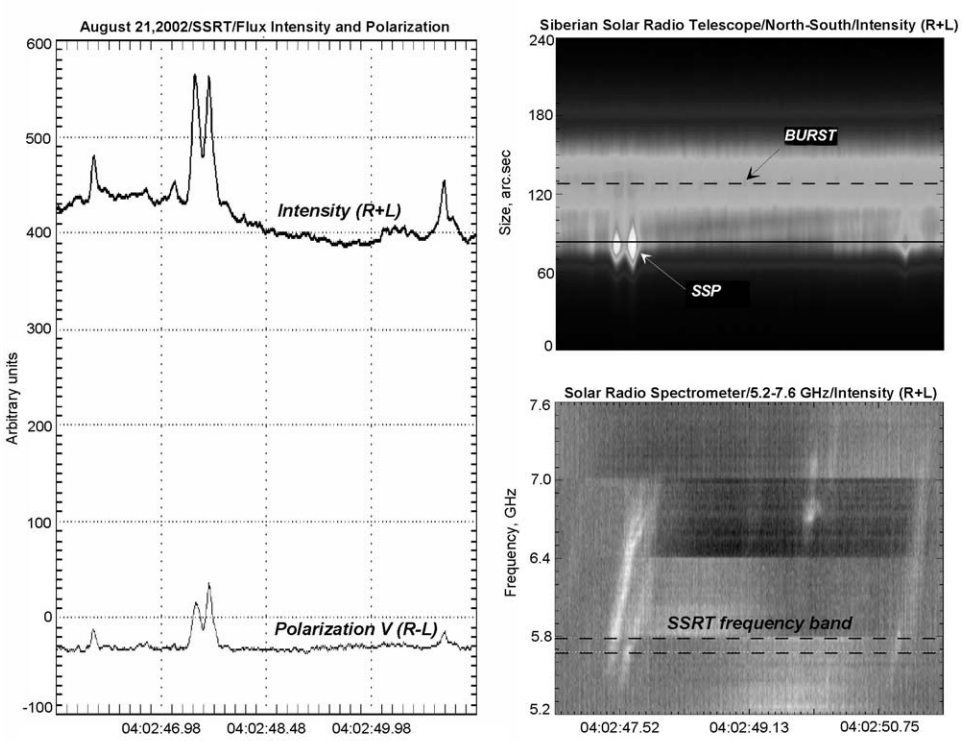

Figure 3. 21 August 2002. *Left:* 1D time profiles in intensity and polarization from SSRT at 5.7 GHz. *Top right:* time development of 1D scans SSRT. *Bottom right:* dynamic spectrum from NAOC.

Nobeyama Polarimeters (1.0–35.0 GHz) showed that there was no response in these cases, i.e., SSP's are narrow band ones.

The first columns present the date, background burst position, and polarization degree of the SSP events. The fifth column presents the signs and values of magnetic field at the MDI magnetograms in the points, corresponding to the brightness centers of the SSP and burst emission in intensity (N – North, and S – South). The label NL corresponds to cases where the distance between the photosphere neutral line and the brightness center of the SSP is less than 10 arc sec. This value is about the error in our procedure of aligning images obtained with the SSRT and the MDI. A next column shows the distances for cases with larger values. The last two columns present the mode emission of the burst and SSP. The burst emission mode was determined for all events excepting the cases (marked as NL) where the burst brightness center position is located directly at the photosphere neutral line. In the SSP column the mode was not determined for two events (1D) where observations from only one linear array of the SSRT were available. In the table the SSP events are distributed according to the types of dynamic spectrum and polarization degree. Most of the events correspond to spikes. It is evident from the

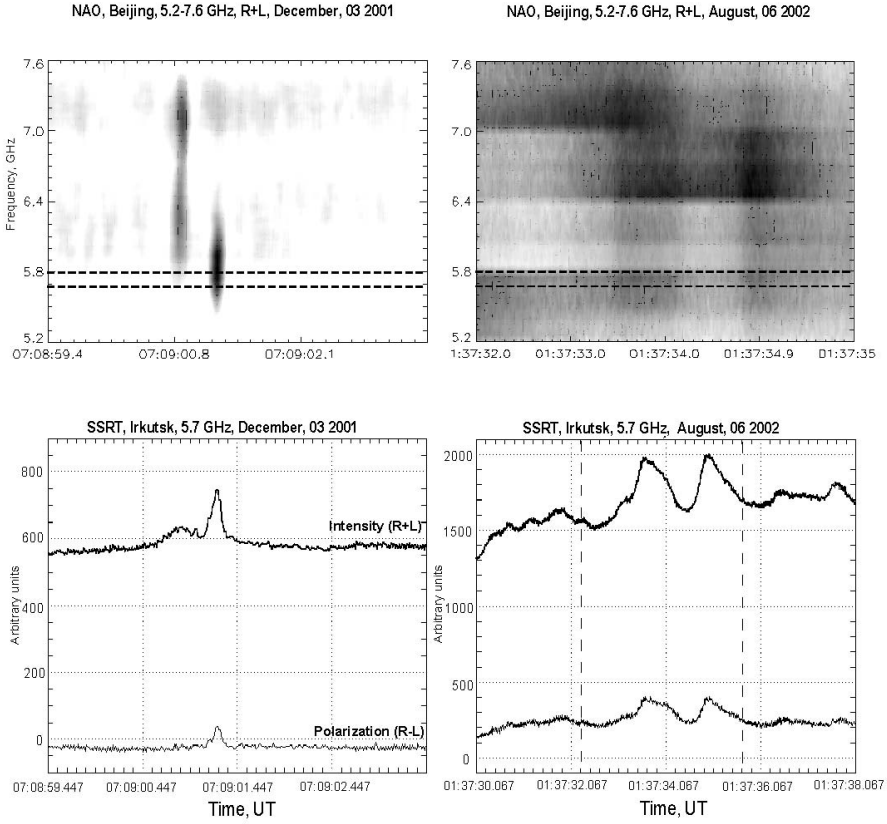

Figure 4. Examples of a broad band and narrow band bursts. *Top:* dynamic spectra from NAOC. *Bottom:* time profiles from SSRT (intensity and polarization). *Bottom right: vertical lines* show the time spans corresponding to the top presented dynamic spectrum.

table that the high degree of polarization can be recorded in the SSP events of every type. Despite the high polarization the photosheric magnetic field under the SSP source does not exceed 250 G. Typically the sources of subsecond pulses are far from AR sunspots with large magnetic fields. Most of the SSP sources are too close to the neutral line that they are less than the aligning error. As a consequence, we can confidently determine the predominant mode of the electromagnetic wave only for events with the large space from the SSP source to the neutral line.

In half the background bursts, the sign of the degree of polarization suggests the extraordinary wave mode. The proportion of this mode increased (75%) if we consider only bursts (12 cases) located well apart from the neutral line. This mode can be generated in an optically thin layer of emitting flare plasma by the gyrosynchrotron mechanism.

TABLE I
Results of observations

No.	Date	Burst position	Degree of polarization, %	Magnetic field SSP/burst, G	Shift of SSP from NL	Burst mode	SSP mode
			Spikes				
1	1 Mar. 2002	S21W08	+75	NL		X	1D
2	27 July 2002	S12E14	+60	90S/550S	10″	X	O
3	13 May 2001	S19W01	+55	NL		X	X
4	3 Dec. 2001	N06W38	+50	NL		X	X
5	16 Dec. 2001	N14W27	−35	NL		O	O
6	27 Dec. 2001	N09W04	−30	130N/2150N	10″	X	O
7	4 Sept. 2002	N09E13	−30	NL		O	X
			Bursts with frequency drift				
8	30 Mar. 2001	N16W21	−75	220N/650N	30″	X	O
9	21 Agu. 2002	S11W47	+45	NL		NL	O
10	17 Sept. 2001	S14E02	+45	35S/450S	20″	X	O
			Broad band bursts				
11	6 Aug. 200206	S07W57	+40	NL		O	O
12	6 Nov. 200106	S23E28	+40	100S/370S	40″	X	O
			With no data on dynamic spectrum				
13	5 Sept. 20015	N14W24	+85	NL		NL	X
14	14 May 200114	S15W11	+80	NL		NL	X
15	0 Sept. 20019	S21W15	+50	NL		NL	1D
16	8 Nov. 200107	S19W05	+40	NL		NL	O
17	22 Oct. 20012	N18W13	+35	40N/NL	10″	NL	X
18	7 July 200207	S17W20	+30	NL		X	O

The SSP are polarized, as a rule, in the sense of an ordinary wave. The proportion is 62.5% for 16 events where the signals for both scanning directions were recorded. If we consider the SSP sources located well apart from a neutral line (6 events), this proportion will increase to 83%. Note that the source positions of the SSPs, recorded in the same flare, are close to one another, and no reversal of the SSP polarization was observed in this case.

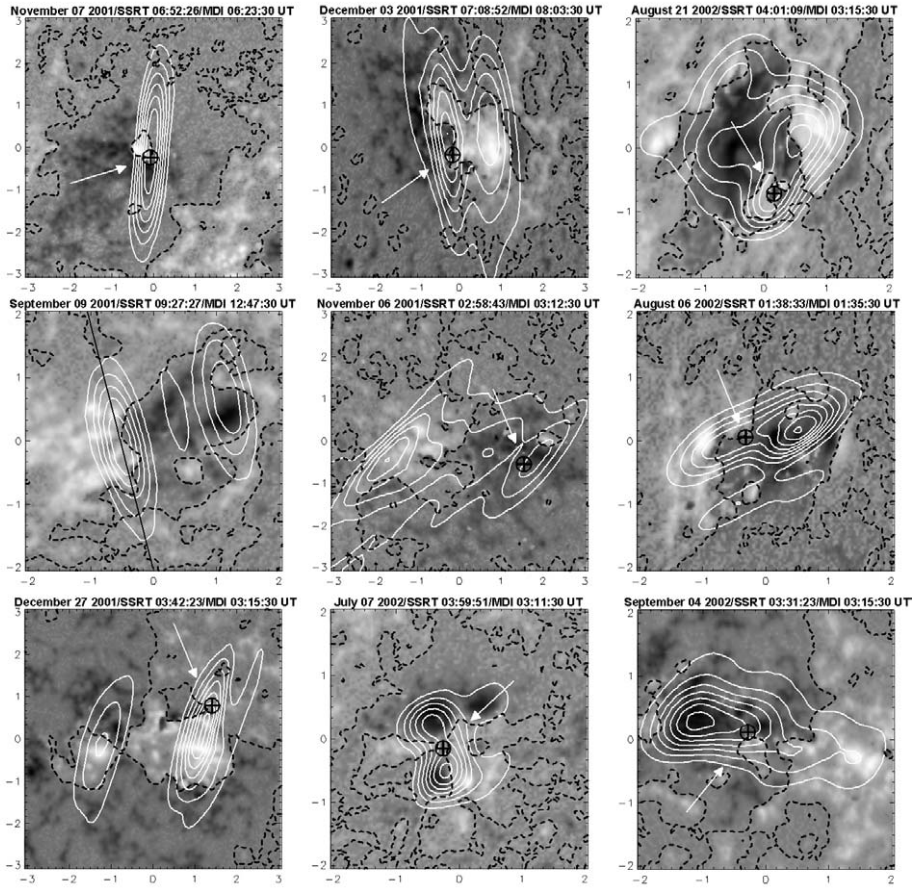

Figure 5. The superposition of SSRT radio maps and MDI magnetograms for our events. *Crosses in circle* show radio SSP sources. *Arrows* indicate SSP. White contours show the brightness temperatures in the intensity $(R + L)$ of 2D SSRT. *Dashed line* is a neutral line of the photospheric magnetic field. *Solid black line* indicates one linear interferometer. Scale ù- arc min, north on the top.

5. Discussion

We conclude that the subsecond pulses with a broad-band spectrum (see Table 1, and Figure 4) are produced by gyrosynchrotron emission generated by a short-duration beam of non-thermal electrons being precipitated into the lower layers of the transition region. This mechanism has been discussed by Kosugi et al. (1988) for the case of short-duration, broadband pulses at frequencies up to 17 GHz, and was suggested by Altyntsev et al. (2000) for interpretation of the subsecond pulses observed at 5.7 and 17 GHz simultaneously. The analysis of the events made in this paper showed that SSP in the cm-waves can be generated by directly precipitating

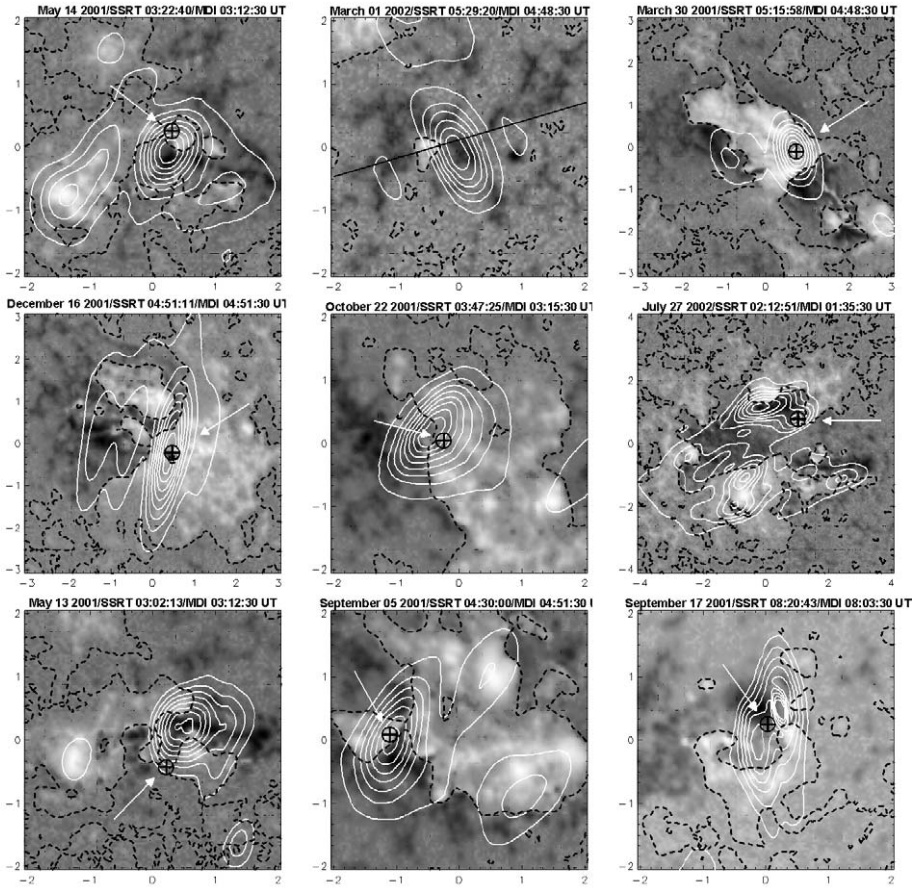

Figure 6. The same as Figure 5.

100–200 keV electrons in tiny regions close to footpoints. The polarization degree did not exceed 20% for these events.

In the other types of SSP where a narrow spectral band was observed (spikes and drifting bursts), it is customary to interpret the emission in terms of coherent mechanisms of emission. Currently the universally accepted mechanisms for SSPs are the electron-cyclotron maser and plasma mechanisms. Interpretation in terms of the maser is in conflict with observations. As a rule, the SSP sources are well apart of the strong magnetic field, and the SSP emission corresponds not less than 5–10 cyclotron frequency harmonic, if we take the value of magnetic field at the photospheric level. At such high harmonics the maser mechanisms are not effective (Fleishman and Melnikov, 1998).

A high degree of polarization would be expected for emission at frequencies close to the Langmuir frequency. In this case the plasma density in the SSP source must be about 4×10^{11} cm^{-3}. The problem is how the plasma oscillations convert

to the electromagnetic wave, and the emission escapes from the source to the outer corona. One of the latest suggestions was made by Chernov *et al.* (2001) that the necessary conditions can be realized at the flare shock fronts propagating from magnetic reconnection regions. A shock wave can ensure high plasma density in the SSP source.

Difficulties emerge in this case, however, because the observed degree of polarization at 5.7 GHz is typically not high. It is necessary to assume effective mechanisms of depolarization along the propagation path of emission in the solar corona. So, we believe that the emission at the double Langmuir frequency due to coalescence of the electrostatic waves is preferable, because the required plasma density is by a factor of four lower, and the absorption effectiveness drops in this case by a factor of 16 (Benz, 1986).

In this case the O-mode must be excited mostly according to Melrose (1987) and Willes and Melrose (1997).

The estimated degree of polarization is determined by Ω_e/ω – ratio of the electron cyclotron frequency to the plasma frequency. With reasonable assumptions about the magnetic field magnitude and the energy of emitting electrons it can reach the value 30%.

We believe that the degree of polarization in the sense of the O-mode can increase considerably along the propagation path of electromagnetic radiation from the SSP source. The polarization degree depends on the conditions in the plasma, surrounding the SSP source. The flux absorption may be represented as $\mathrm{F}^{o,x} = F_0^{o,x} \exp[-\tau/(1 \pm \Omega_e/\omega)]$ (Zhelezniakov, 1969), where the top index corresponds to the wave mode (o – ordinary/x – extraordinary), $F_0^{o,x}$ is the primary wave flux, Ω_e is the cyclotron frequency, ω is the receiving frequency, τ is the optical thickness without a magnetic field, and $\tau = 0.33(T/10^6\ \mathrm{K})^{-3/2}\ X/10^8$ cm, where T is plasma temperature, and X is the scale of plasma density decreasing from the SSP source. Thus, with reasonable ratios $\Omega_e/\omega = 0.1$-0.2, after traveling the thickness $\tau = 5$ (the scale of decrease in density 15 000 km), the degree of polarization in terms of the O-mode increases from 30 to 85%. Using the barometric formula it is possible to estimate the plasma temperature at 3×10^5 K, which is in agreement with the estimates made by Aschwanden (2002).

The absorption in the low corona is an effect of great importance or observations of microwave subsecond pulses. Benz, Magun, and Stehling (1992) concluded that the usual escape condition ($\tau \leq 1$) can been achieved for the source represented by thin fiber filled with relatively dense plasma. In this case the polarization effect is very weak.

We believe that the emission power of the SSP can be sufficiently large (larger by two orders of magnitude (since $\tau = 5$) than without the effect of absorption) in order to be detected at the Earth after the wave has propagated along several optical depths. In this case the observed SSP must be strongly polarized in the O-mode sense and have a large emission anisotropy depending on the spatial distribution of plasma density and temperature around the SSP source. It can explain the rareness

and irregularity of the microwave SSP observations in flare events. Sometimes we can observe not the source directly, but its reflection from the lower layers of corona (Altyntsev *et al.*, 2003b).

6. Conclusion

Our superposition of SSRT radio maps and MDI magnetograms has shown that SSP radio sources typically lie above the polarity inversion line of the active region magnetic field. Such an arrangement indicates that SSP sources, as a rule, are located at the tops of magnetic loops.

In SSP bursts, with the sign of the magnetic field in their sources being beyond question, the ordinary mode of electromagnetic radiation is recorded. In some cases it is not possible to determine the predominant mode of the electromagnetic wave using the sign of the photospheric magnetic field in the region where the SSP source is projected onto the photosphere, because SSP sources are very close to the neutral line, and the accuracy of our superposition was not sufficient (10 arc sec).

Our statistical analysis demonstrates that our results of determining the electromagnetic wave mode in the microwave range do not contradict the Leading Spot Rule.

Observational data lead us to conclude that SSPs are generated by the plasma mechanism of emission at the double plasma frequency. If it is assumed that the emission frequency of 5.7 GHz equals the double plasma frequency, then the plasma density in the SSP source is 10^{11} cm^{-3}.

The high degree of polarization that is recorded on the ground, can be obtained by taking into account the stronger absorption of the X-mode in the plasma surrounding the SSP source in the magnetoactive solar corona.

Acknowledgements

We thank the referee, K. Tapping, very much for his very important and useful comments which helped to improve this paper. We are grateful to Dr Lesovoi for providing us with the SSRT data on subsecond pulses, and to Mr. Mikhalkovsky for his assistance in preparing the English version of the manuscript. This work was supported by Russian projects of RFBR No. 02-02-39030, 03-02-16591, 03-07-90054, and 03-02-16229, NSH-477.2003.2, Vuz grant (E02-3.2-489), *Integratsiya* project No. I0208, *Astronomiya*, Chinese grant G2000078403, and NSFC 102-253-13.

References

Altyntsev, A. T., Grechnev, V. V., and Konovalov, S. K.: 1996, *Astrophys. J.* **469**, 976.

Altyntsev, A. T., Nakajima, H., Takano, T., and Rudenko G. V.: 2000, *Solar Phys.* **195**, 401.

Altyntsev, A. T., Kuznetsov, A. A., Meshalkina, N. S., and Yan Yihua: 2003a, *Astron. Astrophys.* **411**, 263.

Altyntsev, A. T., Lesovoi, S. V., Meshalkina, N. S., Sych R. A., and Yan Yihua: 2003b, *Astron. Astrophys.* **400**, 337.

Aschwanden, M. J.: 2002, *Space Sci. Rev.* **101**, 1.

Benz, A. O.: 1986, *Solar Phys.* **104**, 99.

Benz, A. O. and Güdel, M.: 1987, *Solar Phys.* **111**, 175.

Benz, A. O., Magun, A., Stehling, W., and Su, H.: 1992, *Solar Phys.* **141**, 335.

Chernov, G. P., Fu, Q. J., Lao D. B., and Hanaoka Y.: 2001, *Solar Phys.* **201**, 153.

Dulk, G. A.: 1985, *Astron.Astrophys.* **23**, 169.

Gudel, M. and Zlobec, O.: 1991, *Astron. Astrophys.* **245**, 299.

Fleishman, G. D. and Melnikov, V. F.: 1998, *Physics-Uspekhi* **41**, 1157.

Fu, Q., Qin, Z., Ji, H., and Pei, L.: 1995, *Solar Phys.* **160**, 97.

Grechnev, V. V., Lesovoi, S. V., and Smolkov, G. Ya. *et al.*: 2003, *Solar Phys.* **216**, 239.

Ji, H., Fu, Q., Liu, Y., Cheng, C., and Chen, Z.: 2003, *Solar Phys.* **213**, 359.

Kosugi, T., Dennis, B. R., and Kai, K.: 1988, *Astrophy. J.* **324**, 1118.

Lesovoi, S. V. and Kardapolova, N. N.: 2003, *Solar Phys.* **216**, 225.

Melrose, D. B.: 1987, *Solar Phys.* **111**, 89.

Meshalkina, N. S., Altyntsev, A. T., Grechnev, V. V., Sych, R. A., and Yan Yihua: 2002, *The 10th European Solar Phys. Meeting* **1**, 343.

Smolkov, G. Ya., Pistolkors, A. A., Treskov, T. A. *et al.*: 1986, *Astrophys. Space Sci.* **119**, 1.

Platonov, K. Yu. and Fleishman, G. D.: 2002, *Physics-Uspekhi* **45**, 235.

Willes, A. J., and Melrose, D. B.: 1997, *Solar Phys.* **171**, 393.

Zhelezniakov, V. V.: 1969, *Radio Emission of the Sun and Planets*, 1st ed. Pergamon Press, Oxford.